Characterization of Intrinsic Amorphous Hydrogenated Silicon as a Thin-Film Photocathode Material. Efficient Photoreduction Processes in Aqueous Solution

D. Jed Harrison,[1] Gary S. Calabrese,[1] Antonio J. Ricco,[1] Joseph Dresner,[2] and Mark S. Wrighton*[1]

Contribution from the Department of Chemistry, Massachusetts Institute of Technology, Cambridge, Massachusetts 02139, and RCA Laboratories, David Sarnoff Research Center, Princeton, New Jersey 08540. *Received January 13, 1983*

Abstract: Intrinsic amorphous hydrogenated silicon, a-Si:H, has been characterized as a thin-film (8000 Å) a-Si:H material. The intrinsic a-Si:H is deposited onto a 200-Å thick, heavily B-doped, layer of a-Si:H on stainless steel. The 200-Å p^+-a-Si:H layer ensures a back contact to the valence band to give as large a field across the 8000-Å intrinsic layer as possible when the intrinsic layer is contacted on the other side by an electrolyte solution containing a redox couple. The a-Si:H photocathodes give good photovoltages in aqueous and nonaqueous media, up to 855 mV, depending on the $E_{1/2}$ of the redox couple in contact with the electrode. A plot of photovoltage vs. $E_{1/2}$ shows a slope of only 0.42. A zero photovoltage is extrapolated to obtain for $E_{1/2}$ no more negative than +0.9 V vs. SCE; the photovoltage is constant for $E_{1/2}$ more negative than ~−0.8 V vs. SCE. The slope of less than 1.0 suggests a deleterious role for states situated between the valence and conduction bands of a-Si:H. The surface of a-Si:H can be derivatized with an *N,N'*-dialkyl-4,4'-bipyridinium reagent followed by deposition of Pd or Pt to effect H_2 evolution at an electrode potential up to ~700 mV more positive than on a conventional electrode. The durability and photovoltage of a-Si:H photocathodes are superior to those of single-crystal p-Si photocathodes, but the wavelength response, rectangularity of current–voltage curves, and the quantum yield for electron flow offset the advantages of the thin-film photocathode. The sustained energy conversion efficiency for 632.8-nm light to electricity or H_2 is about the same for a-Si:H and single-crystal p-Si under the same conditions. Importantly, constant output of electricity for 50 h at ~3.2 mA/cm^2 has been obtained from a-Si:H photocathode-based cells employing an aqueous $Eu^{3+/2+}$/KCl redox couple/electrolyte combination.

Introduction

Amorphous hydrogenated silicon, a-Si:H, is a material of considerable interest for photovoltaic applications. Large area devices can be prepared in thin-film form on inexpensive substrates in a continuous fashion; the material is derived from abundant elements; and the spectral response is reasonably well matched to the solar spectrum.[3] We have recently reported on the use of intrinsic a-Si:H as a photoanode in nonaqueous electrolyte solutions.[4] The optical to electrical energy conversion efficiencies of ~4.5% were found to be comparable to single-crystal n-Si under the same conditions, and the intrinsic a-Si:H photoanode-based cells give constant output for more than 100 h in $C_2H_5OH/[n\text{-}Bu_4N]ClO_4$ solutions containing ferricenium/ferrocene. In aqueous solution a-Si:H photoanodes give good photovoltages, but undergo oxidative decomposition,[4,5] a problem common to many small band gap n-type semiconductors.[6] Generally, photocathode materials are more resistant to corrosion in aqueous systems as photogenerated holes, h^+, are swept away from the solution/electrolyte interface by the electric field at the interface, thus protecting the surface from the strongly oxidizing h^+'s.

The energetics of a device employing an intrinsic a-Si:H photocathode are represented in Scheme I.[4] To behave as an efficient cathode the intrinsic material should be contacted as close as possible to the valence band edge, E_{VB}, by the back contact layer. In the present work, this has been accomplished by first depositing a thin layer (200 Å) of p^+-a-Si:H onto the metal contact. The deposition of a thick-layer (8000 Å) of intrinsic a-Si:H onto the p^+ layer completes the assembly. At the electrode/electrolyte interface, contact by sufficiently negative redox couples, A^+/A, will then result in a field across the insulating a-Si:H film in the dark, as shown in Scheme I. Upon illumination with light of energy greater than the band gap, E_g, the film becomes conducting and the field drives photogenerated h^+'s toward the back contact, while the e^-'s are driven to the solution.

Scheme I. Representation of the Interface Energetics of a Stainless Steel/p^+-a-Si:H/Intrinsic a-Si:H/Liquid Electrolyte Interface[a]

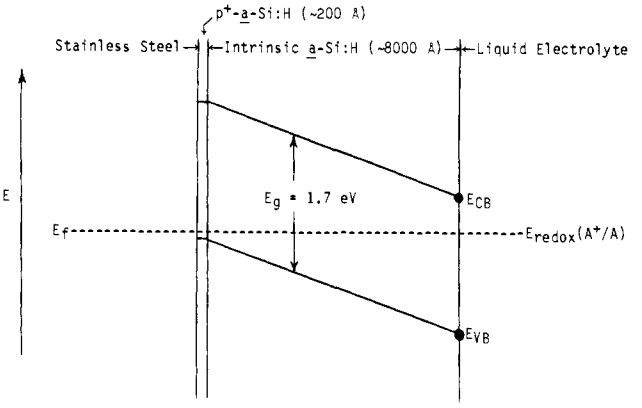

[a] The difference in E_{VB} and E_{redox} is the maximum open-circuit photovoltage. In this study an open-circuit photovoltage of ~850 mV is obtained for E_{redox} more negative than −0.8 V vs. SCE.

In this paper, we report the first use of intrinsic a-Si:H as an efficient photocathode. A prior report[7] regarding p-type a-Si:H as a photocathode suggests that poor output parameters would be found for a-Si:H photocathodes. It has been found that doping of a-Si:H increases the recombination rate of photogenerated $e^- - h^+$ pairs,[3a,8] suggesting intrinsic materials would be more de-

(1) Massachusetts Institute of Technology.
(2) RCA.
(3) (a) Carlson, D. E.; Wronski, C. R.; Pankove, J. I.; Zanzucchi, P. J.; Staebler, D. L. *RCA Rev.* **1977**, *38*, 211. (b) Fritzche, H.; Tsai, C.C.; Persons, P. *Solid State Technol.*, **1978**, *21*, 55. (c) Greeb, K. H.; Fuhs, W.; Mell, H.; Welsch, H. M. *Solar Energy Mater.* **1982**, *7*, 253.
(4) Calabrese, G.S.; Lin, M.-S.; Dresner, J.; Wrighton, M. S. *J. Am. Chem. Soc.* **1982**, *104*, 2412.
(5) (a) Williams, R. *Appl. Phys.* **1979**, *50*, 2848. (b) Ayers, W. M. *J. Appl. Phys.* **1982**, *52*, 6911. (c) Skotheim, T.; Lunstrom, I.; Delahoy, A. E.; Kampas, F. J.; Vanier, P. E. *Appl. Phys. Lett.* **1982**, *40*, 281.
(6) (a) Bard, A. J.; Wrighton, M. S. *J. Electrochem. Soc.* **1977**, *124*, 1706. (b) Gerischer, H. *J. Electroanal. Chem. Interfacial Electrochem.* **1977**, *82*, 133. (c) Park, S.-M.; Barber, M. E. *Ibid.* **1979**, *99*, 67.
(7) Ayers, W. M. *J. Electrochem. Soc.* **1982**, *129*, 1644.

0002-7863/83/1505-4212$01.50/0

sirable. In addition, since the width of the space charge layer depends on the carrier density, the use of intrinsic material results in an electric field, which separates photogenerated carriers, throughout most of the bulk of the intrinsic layer.[3a] The a-Si:H photocathode-based devices described here compare favorably with devices previously reported[9] based on single-crystal p-type Si in terms of efficiency and durability.

Under illumination, the key is that the flow of current corresponding to the reduction of A^+ (cf. Scheme I) can occur for photoelectrode potentials, E_f, that are more positive than $E_{redox}(A^+/A)$. The extent to which the potential onset of current flow is more positive than $E_{redox}(A^+/A)$ is the photovoltage, E_V. We report below values of E_V as high as 855 mV, rivaling the best single-crystal photocathode materials such as p-InP,[10] p-WSe_2,[11] and p-WS_2[12] that have good solar response. The photovoltage for a-Si:H photocathodes exceeds that of single-crystal p-Si[13] by 200–300 mV. Moreover, the best Schottky barrier from intrinsic a-Si:H/M has given an open-circuit photovoltage of ~850–900 mV.[3]

Our data for E_V show that intrinsic a-Si:H should be a good photocathode for reducing H_2O to H_2. However, there is no expectation that the surface of a-Si:H would be "good" for H_2 generation, since H_2 evolution is typically associated with large overvoltages. The a-Si:H, like single-crystal Si, though, has surface functionality that should allow attachment of catalyst assemblies for improving the rate of reduction without altering output photovoltage. We and others have shown that various surface modification procedures can be used to improve H_2 evolution efficiency from photocathodes.[9,14] Covalent attachment of reagent I to the a-Si:H surface by hydrolysis results in a surface-confined,

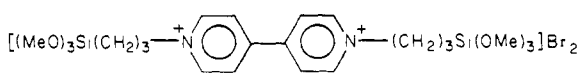

I

electroactive polymer, $[(PQ^{2+/+})_n]_{surf}$. Electrodeposition of Pd or Pt metal onto the polymer completes a structured interface where the surface of the photoelectrode is separated by the polymer from the metallic catalyst.[9b] Such modified a-Si:H photocathodes give optical to electrical energy conversion efficiencies for H_2 evolution close to those obtained at similarly modified single-crystal p-Si electrodes.[9] Direct platinization of the a-Si:H surface has also been employed, and is found to significantly enhance the rate of H_2 evolution as found for single-crystal photocathodes.[14]

Experimental Section

Electrodes. The a-Si:H sample was synthesized by the DC glow discharge technique[3] and consisted of a B-doped p^+-a-Si:H layer (~200 Å) contacting a stainless steel substrate followed by 8000 Å of undoped intrinsic a-Si:H. The material used has the same optical and electronic properties as material previously synthesized and characterized.[3] The B-doped layer was synthesized using a glow discharge technique with SiH_4 and B_2H_6. The intrinsic layer was formed using only SiH_4 in the glow discharge. Two samples, ~3 in. × 3 in., were cut into electrode size pieces. The electrodes were ~0.25 cm^2 and were fashioned as in our previous report on a-Si:H photoanodes.[4] An aqueous 5% HF etch was employed for 10 to 30 s prior to use to remove excess surface oxide and yield reproducible photoeffects.

Chemicals. HPLC grade (Baker) CH_3CN was distilled from P_2O_5. The $[n\text{-}Bu_4N]BF_4$ (Southwestern Analytical Chemicals) was vacuum dried at 50 °C for 24 h. Water was distilled and deionized; other reagents and redox couples are commerically available or have been synthesized and used previously in related studies.[4,10b,12,13,15] *N,N'*-Bis(3-propylsulfonate)-4,4'-bipyridinium (PVS) was prepared by a modification of a published procedure.[16] Anhydrous 4,4'-bipyridine (Eastman Chemicals, 10 g, 64 mmol) was added to 300 mL of distilled CH_3CN and refluxed with 1,3-propanesultone (Sigma, 19.5 g, 160 mmol) for 3 h. The solvent was then stripped off under vacuum, and the off-white solid was taken up in a minimum of hot water, then precipitated with C_2H_5OH to purify. the precipitate was rinsed with C_2H_5OH, then $(C_2H_5)_2O$, and dried under vacuum: yield 17 g (66%); ^1H NMR (Varian T-60, D_2O, δ to external Me_4Si) 8.82 (8 H, q), 4.93 (4 H, t), 2.80 (8 H, m).

Equipment and Procedures. Cyclic voltammograms were recorded in Ar- or N_2-purged C_2H_5OH or CH_3CN/0.1 M $[n\text{-}Bu_4N]BF_4$ or H_2O/0.1 M KCl solutions with redox reagents present at ~1 mM in the nonaqueous solvents and ~5 mM in H_2O. High ionic strength (μ = 0.5 M), appropriately buffered solutions (phosphate, acetate, chloroacetate) or sulfuric acid was used to measure effects of pH variation. The electrochemical equipment has been described elsewhere.[4,9] A single-compartment, three-electrode cell was used with a Pt counterelectrode and saturated calomel reference electrode (SCE). Electrodes were illuminated with a beam-expanded 632.8-nm He–Ne laser (Aerotech) at ~40 mW/cm^2 or the visible lines of an Ar ion laser (Spectra Physics Model 164). A Viewlex film strip projector with a 350-W tungsten source was IR filtered through a 10-cm-long H_2O-filled lens to provide a source of white light at up to 250 mW/cm^2. Intensities were varied using Schott neutral density filters (NG5, NG9, and NC4) and were measured with a Tektronix J16 radiometer equipped with a J6502 probe. High-intensity white light was measured with a Solarex reference cell (Solarex) which was calibrated to within 10% against the Tektronix radiometer using the Schott filters. The photoaction spectra were acquired with a Pine RDE 3 potentiostat and a PAR Model 6001 photoacoustic spectrometer, as has been detailed previously.[15] Spectra were recorded in 0.5 M $EuCl_3$, 0.5 M KCl solution at pH ~4 with the photocathode at −0.4 or −0.8 V vs. SCE. Photoacoustic spectra were taken using the same spectrometer.

Steady-state current–voltage curves were obtained in single-compartment, three-electrode cells, at 5 or 10 mV/s. Solutions were first poised by reduction or oxidation of the redox couple in a two-compartment cell and E_{redox} was measured at a Pt or Ag electrode. Solutions were stirred to ensure light intensity limited currents. For the H_2 evolution stability run, doubly distilled, deionized H_2O was used to make a solution 1 mM in Baker Ultrex H_2SO_4, 0.1 M Na_2SO_4 (Baker, reagent). The solution was purged with H_2 passing over a Pt wire to act as a reference and was preelectrolyzed with a C cathode to remove reducible metallic impurities. The quartz glassware used was pretreated in 1 M HNO_3 at 80 °C for several hours, followed by the same treatment in 1 M HCl. Rinsing and then soaking 24 h in doubly distilled, deionized water completed the procedure.

Electrodes were derivatized with reagent I by repeated cycling through the first reduction wave in an aqueous solution of ~3 mM I, 0.1 M KCl, 0.2 M K_2HPO_4, or by potentiostatting negative of the first reduction wave of I (~−0.65 V vs. SCE). Metallization of the derivatized or naked[9a] electrode surface was effected by photoelectrochemical reduction of K_2MCl_4 (M = Pd, Pt). The a-Si:H/$[(PQ^{2+})_n]_{surf.}$ electrode was potentiostated to ~+0.1 V vs. SCE in pH 4 solution and illuminated with white light (~200 mW/cm^2). A small amount (~5 μM) of MCl_4^{2-} was added to the solution at which point the current increases as M is deposited and catalyzes H_2 evolution. When the current ceased to increase, the electrode was withdrawn from the solution and rinsed liberally with pH 4 aqueous electrolyte containing no MCl_4^{2-}. The a-Si:H/$[(PQ^{2+})_n/M]_{surf.}$ electrode was then studied in solutions containing no MCl_4^{2-}.

The Auger/depth profile analyses were obtained as previously described.[9] Charging of the intrinsic a-Si:H was avoided by illumination of the sample face with 632.8-nm or white light directed through the

(8) (a) Moore, A. R. *Appl. Phys. Lett.* **1977**, *31*, 762. (b) Kuwano, Y.; Tsuda, S.; Ohnishi, M. *Jpn. J. Appl. Phys.* **1982**, *21*, 235.
(9) (a) Dominey, R. N.; Lewis, N. S.; Bruce, J. A.; Bookbinder, D. C.; Wrighton, M. S. *J. Am. Chem. Soc.* **1982**, *104*, 467. (b) Bruce, J. A.; Murahashi, T.; Wrighton, M. S. *J. Phys. Chem.* **1982**, *86*, 1552. (c) Bruce, J. A.; Wrighton, M. S. *Isr. J. Chem.* **1982**, *22*, 184.
(10) (a) Heller, A.; Miller, B.; Lewerenz, H. J.; Bachman, K. J. *J. Am. Chem. Soc.* **1980**, *102*, 6555. (b) Dominey, R. N.; Lewis, N. S.; Wrighton, M. S. *Ibid.* **1981**, *103*, 1261.
(11) Nagasubramanian, G.; Bard, A. J. *J. Electrochem. Soc.* **1981**, *128*, 1055.
(12) Baglio, J. A.; Calabrese, G. S.; Harrison, D. J.; Kamieniecki, E.; Ricco, A. J.; Wrighton, M. S.; Zoski, G. D. *J. Am. Chem. Soc.*, **1983**, *105*, 2246.
(13) Bocarsly, A. B.; Bookbinder, D. C.; Dominey, R. N.; Lewis, N. S.; Wrigton, M. S. *J. Am. Chem. Soc.* **1980**, *102*, 3683.
(14) (a) Nakato, Y.; Tonomura, S.; Tsubomura, H. *Ber. Bunsenges. Phys. Chem.* **1976**, *80*, 1289. (b) Kautek, W.; Gobrecht, J.; Gerischer, H. *Ibid.* **1980**, *84*, 1034. (c) Heller, A.; Vadimsky, R. G. *Phys. Rev. Lett.* **1981**, *46*, 1153. (d) Lewerenz, H. J.; Aspnes, D. E.; Miller, B.; Malm, D. L.; Heller, A. *J. Am. Chem. Soc.* **1982**, *104*, 3325. (e) Heller, A.; Aharon-Shalom, E.; Bonner, W. A.; Miller, B. *Ibid.* **1982**, *104*, 6942.
(15) Baglio, J. A.; Calabrese, G. S.; Kamieniecki, E.; Kershaw, R.; Kubiak, C. P.; Ricco, A. J.; Wold, A.; Wrighton, M. S.; Zoski, G. D. *J. Electrochem. Soc.* **1982**, *129*, 1461.
(16) (a) Willner, I.; Degani, Y. *J. Chem. Soc., Chem. Commun.* **1982**, 761. (b) Willner, I.; Degani, Y. *Isr. J. Chem.* **1982**, *22*, 163.

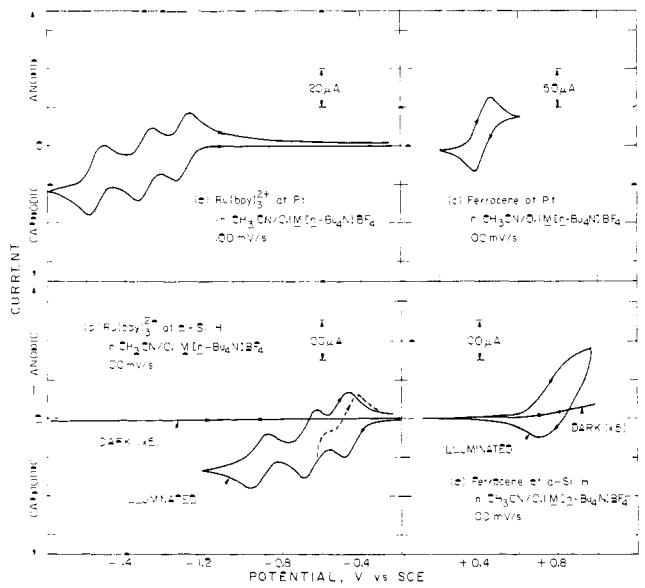

Figure 1. Comparison of the cyclic voltammetry of 1 mM solutions of two redox couples at Pt and intrinsic a-Si:H photocathodes. Illumination is with white light (200 mW/cm^2).

sample viewing port. Scanning electron micrographs were obtained on an AMR Model 1000A equipped with a Tracor Northern Model T-N2000 energy dispersive X-ray analyzer, using a 20-keV electron beam. Electrodes were mounted as samples using copper tape and graphite paint. Gold coating of the samples was unnecessary.

Results and Discussion

The a-Si:H material used in this study is the same as that reported previously and is essentially intrinsic. The Fermi level lies about 0.8 eV below the bottom of the conduction band[4] and the direct optical transition is about 1.7 eV.[3] However, in this case the contact to the intrinsic a-Si:H is provided by a thin layer (~200 Å) of heavily B-doped p$^+$-a-Si:H on the stainless steel substrate to contact the valence band (Scheme I). The electrodes block the flow of current in the dark, consistent with the intrinsic nature of the 8000-Å thick layer of a-Si:H. Visible-light irradiation of the electrode provides sufficient conductivity to allow its use in photoelectrochemical experiments. The p$^+$-a-Si:H contact layer insures its role as a photoelectrode capable of effecting uphill reductions with the maximum photovoltage.

Interfacial Energetics. The electron-transfer kinetics and interfacial energetics of a-Si:H photocathodes have been explored using nonaqueous solutions of fast, one-electron, outer-sphere electron-transfer reagents, as done previously for a-Si:H photoanodes.[4] Whether reduction of a redox species will occur at a potential positive of that at a reversible electrode depends on the potential of the couple, $E_{1/2}$, and the position of the flat band potential, E_{FB}, of the photocathode. Results with a-Si:H photoanodes place the conduction band edge, E_{CB}, at ~−0.7 V vs. SCE in CH_3CN.[4] For an E_g of ~1.7 eV this puts the valence band edge, E_{VB}, at ~+1.0 V vs. SCE. Thus, a-Si:H photocathodes should be capable of effecting photoassisted uphill reductions over a large potential regime (negative of ~+1.0 V vs. SCE).

The response of the intrinsic a-Si:H to redox couples lying near the extremes of the nearly 2-V potential range examined in CH_3CN is illustrated in Figure 1. In the dark the electrode shows negligible current for both oxidation and reduction, while under illumination well-defined cyclic voltammograms for a large number of redox couples can be observed (Figure 1 and Table I). In contrast to illuminated a-Si:H photoanodes and Pt electrodes for which the response to $Ru(bpy)_3^{2+/+/0}$ appears reversible, the a-Si:H photocathodes give >800 mV of photovoltage, E_V, for each of the three one-electron reductions of the couple, where E_V is taken as the difference between the reduction current peak potential at Pt and at a-Si:H. The highest E_V observed is ~855 mV. At the positive extreme, oxidation of the a-Si:H surface competes with heterogeneous electron transfer to redox species in solution, as indicated by the broadened wave observed for ferrocene (Figure 1d). Repeated scanning through this wave results in a passivated surface after about five scans, and occurs even more rapidly when more positive couples are examined.

We have investigated the response of a number of redox couples and find that any couple having $E_{1/2}$ negative of ~+0.7 V vs. SCE can be observed to be reduced in a thermodynamically uphill fashion at a-Si:H photocathodes (Table I). The onset of reductive current for acetylferrocene shows that E_{FB} must be positive of ~+0.9 V vs. SCE in CH_3CN. Examination of more positive couples is unfortunately precluded by current associated with electrode oxidation. However, the lower limit for E_{FB} is consistent with the position of E_{CB} determined for a-Si:H photoanodes.[4] As shown in Figure 2 there is a systematic variation of E_V with $E_{1/2}$

Table I. Comparison of a-Si:H Photocathodes with Pt by Cyclic Voltammetry

redox couple (no.)[a]	$E_{1/2}$ at Pt (V vs. SCE)[b]	E_V, mV[c]
$[Ru(2,2'\text{-bipyridine})_3]^{0/-}$ (1)	−1.75	835
$[BAQ]^{-/2-}$ (2)	−1.51	600
$[Ru(2,2'\text{-bipyridine})_3]^{+/0}$ (3)	−1.50	845
$[Ru(2,2'\text{-bipyridine})_3]^{2+/+}$ (4)	−1.31	850
[N,N'-bis(3-propylsulfonate)-4,4'-bipyridinium]$^{-/2-}$ (5)[d]	−1.03	850
$[BAQ]^{+/-}$ (6)	−0.93	600
$[MV]^{+/0}$ (7)	−0.83	825
$[Ru(acac)_3]^{-/2-}$ (8)	−0.75	770
[N,N'-bis(3-propylsulfonate)-4,4'-bipyridinium]$^{0/-}$ (9)	−0.63	680
$[MV]^{2+/+}$ (10)	−0.42	700
$[TCNQ]^{-/2-}$ (11)	−0.35	385
[decamethylferrocene]$^{+/0}$ (12)	−0.09	535
[pentamethylferrocene]$^{+/0}$ (13)	+0.15	480
$[TCNQ]^{0/-}$ (14)	+0.21	140
[ferrocene]$^{+/0}$ (15)	+0.41	340
[acetylferrocene]$^{+/0}$ (16)	+0.65	230

[a] Data are for CH_3CN/0.1 M $[n\text{-}Bu_4N]BF_4$ solutions at 25 °C, 100 mV/s, except couples 5 and 9 which are in unbuffered H_2O/0.1 M KCl. Numbers are keyed to Figure 2. BAQ is 2-*tert*-butyl-9,10-anthraquinone; MV is N,N'-dimethyl-4,4'-bipyridinium; acac is acetylacetonate; TCNQ is 7,7,8,8-tetracyanoquinodimethane; pentamethylferrocene is 1,2,3,4,5-pentamethylferrocene. [b] $E_{1/2}$'s were calculated from cyclic voltammetry data according to $E_{1/2} = (E_{PA} + E_{PC})/2$, where E_{PA} and E_{PC} are the anodic and cathodic current peaks, respectively. [c] $E_V = |E_{PC,Pt} - E_{PC,illum\ a\text{-}Si:H}|$. Illumination was provided by a Viewlex projector lamp, W source, at ~200 mW/cm^2. [d] Cyclic voltammogram was obtained at a W wire electrode to avoid H_2 evolution.

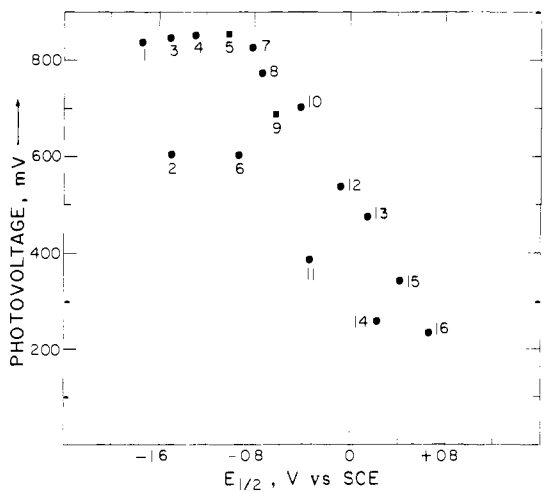

Figure 2. Plot of photovoltage at a-Si:H photocathodes vs. the $E_{1/2}$ of the associated redox couple. Photovoltage is as defined in the text. The individual numbered entries are identified in Table I for aqueous (■) and nonaqueous media (●).

of the redox species in a fashion consistent with expectation.[17] The fact that very negative redox couples (more negative than the E_{CB} position deduced from the E_{FB} value) give photovoltages that are independent of E_{redox} is consistent with the conclusion that the surface is inverted or Fermi level pinned, as has been concluded for other photoanodes.[12,17] The interface does not behave in an ideal manner in that the slope of the curve in the positive E_{redox} regime is less than that predicted by the ideal model, eq 1, for

$$|E_{FB} - E_{redox}| = E_V(oc) \quad (1)$$

E_{redox} negative of E_{FB}. The slope determined for well-behaved couples between −0.9 and +0.6 V vs. SCE is 0.42. It is interesting to compre this value with that found for n^+/i-a-Si:H/M Schottky barrier devices[3a,18] where the barrier height was found to vary with the metal, M, work function for large work-function metals, with a nonideal slope of 0.52. A slope of <1.0 was attributed to the presence of interface states at the Schottky barrier with a density of $\sim 10^{13}$ cm^{-2} eV^{-1}. In aqueous solution n^+/i-a-Si:H photoanodes are reported to yield photovoltages which vary with $E_{1/2}$ of the redox species in solution in a linear fashion with a slope of 0.53.[5a] Unfortunately, these data are vitiated by the fact that oxidation of the surface occurs at positive potentials.[5b] The similarity of these results and those for the a-Si:H/M interfaces with those presented here suggests that the surface, or interface, states have a common source, such as a native surface oxide. A number of other semiconductor photoelectrodes have been examined which depart from ideality because of surface states and chemistry of the interfacial region.[4,10b,13,15,17,19] The a-Si:H is known to have a thin, native oxide of ill-defined stoichiometry that may be responsible for residual interface states.[18]

In some cases specific interactions may occur between a semiconductor surface and a solution species, resulting in a change in the surface kinetics or energetics.[20] Such an interaction is signaled here by the anomalously low E_V obtained for 2-*tert*-butyl-9,10-anthraquinone (BAQ) and the quinone-like molecule tetracyanoquinodimethane (TCNQ). Quinones are known to interact strongly with electrode surfaces, including semiconductors such as GaAs,[21] often resulting in perturbed voltammetry. The nature of the interaction of BAQ and TCNQ with a-Si:H requires further study.

In aqueous media, oxidation of the a-Si:H photocathodes examined here is significant in the presence of redox species with an $E_{1/2}$ positive of $\sim$−0.2 V vs. SCE. The reduction potential of *N*,*N*′-bis(3-propylsulfonate)-4,4′-bipyridinium (PVS) lies more negative than this.[16] The cyclic voltammetry at a-Si:H is well defined and exhibits a photoreduction peak similar in position to that for a surface-confined polymer derived from reagent I (vide infra). The E_V obtained for the two one-electron reductions of PVS in H_2O/0.1 M KCl are close to the values found in CH_3CN/0.1 M $[n\text{-}Bu_4N]ClO_4$ for redox couples having similar potentials (Figure 2, Table I). The similarity of E_V in aqueous and nonaqueous electrolyte suggests no major differences in the band-edge positions in the two media. The cyclic voltammetry of PVS has been examined as a function of pH and the photocathodic peak position shifts from $\sim$−0.08 at pH 9 to $\sim$+0.01 at pH 1, consistent with a shift of the band-edge positions of $\sim$15 mV/pH unit. Single-crystal p-Si shows a small shift with pH variation.[9] We find the a-Si:H photocathodes to be more rugged than crystalline p-Si. In 5 mM aqueous solutions of PVS at $\sim$40-mW/cm^2 illumination the a-Si:H photocathode may be cycled through the two viologen waves to potentials as positive as +0.4 V vs. SCE dozens of times with no change in the response. Crystalline p-Si shows substantial decline in photocurrent after only a few cycles when the anodic limit is +0.4 V vs. SCE, presumably because of surface oxide formation. The relative resistance to oxide growth of a-Si:H compared to Si could be due to the fact that Si-H bonds are stronger than Si–Si bonds, but is more likely a consequence of the more positive E_{FB} for a-Si:H.

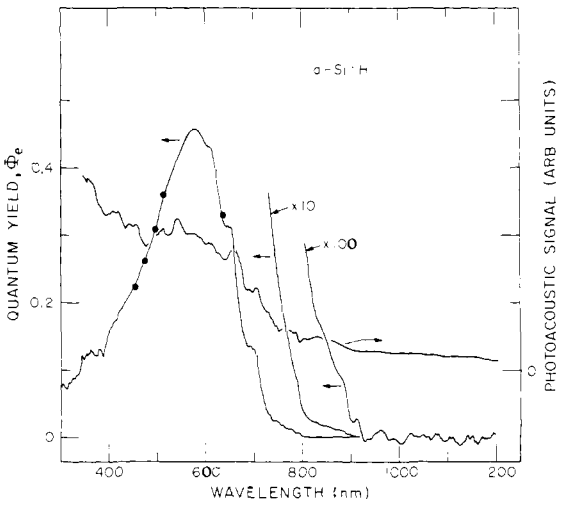

Figure 3. Plot of quantum yield, Φ_e (left axis), vs. wavelength for an a-Si:H photocathode in aqueous 0.5 M $EuCl_3$, 0.5 M KCl, pH 4 solution. Solid curve is taken at −0.4 V vs. SCE with a PAR photoacoustic spectrometer (see Experimental Section) and represents relative quantum yield. Plots (▪) are absolute Φ_e values determined at E_{redox} (−0.57 V vs. SCE) with a monochromatic source (1.5 mW/cm^2). The photoacoustic absorption spectrum (right axis) of powdered a-Si:H/MgO (ratio 1:10) is shown for comparison.

Spectral Response. The photoaction spectrum of a-Si:H photocathodes shows the relative quantum yield for electron flow, Φ_e, vs. wavelength (Figure 3). Values of Φ_e were measured for a photocathode at $E_f = E_{redox}(Eu^{3+/2+})$ in aqueous Cl^- and are included in Figure 3 for calibration purposes. The values of Φ_e measured are uncorrected for reflection losses estimated to be $\sim$30%. Thus, the maximum Φ_e at $\sim$580 nm is $\sim$0.65, the number of electrons detected in the external circuit divided by the number of photons absorbed by the a-Si:H. The onset of photocurrent occurs at $\sim$900 nm (1.4 eV), and there is a pronounced peak at 580 nm, with a decline in Φ_e at shorter wavelengths. The fact that the onset of photoresponse is at lower energy than the direct optical gap is attributable to tailing of states into the gap region. The $Eu^{3+/2+}$ redox couple employed accounts for the structured absorption lines at $\sim$390 nm (0.5 M $EuCl_3$), while Eu^{2+} generated at the electrode surface absorbs light at wavelengths shorter than $\sim$430 nm at the 8-nm resolution used. The shoulders observed in the photoaction spectrum between 600 and 700 nm are likely caused by interferometric effects arising from the thin-film nature of the electrode; such effects have been reported previously with a-Si:H photoelectrodes in aqueous 0.1 M KCl solution.[22] Flooding the sample with white light ($\sim$30 mW/cm^2) while scanning the frequency modulated monochromatic excitation source does not significantly change the spectral response, indicating that a decline in photoconductivity near the back contact, due to decreased light penentration depth for short wavelength light, is not responsible for the reduced quantum yields. For potentials negative of the onset of cathodic current, the plot of relative Φ_e vs. wavelength is independent of the electrode potential.

(17) Bard, A .J.; Bocarsly, A. B.; Fan, F.-R. F.; Walton, E. G.; Wrighton, M. S. *J. Am. Chem. Soc.* **1980**, *102*, 3671.
(18) (a) Wronski, C. R.; Carlson, D. E.; Daniel, R. E. *Appl. Phys. Lett.* **1976**, *29*, 602. (b) Wronski, C. R.; Carlson, D. E. *Solid State Commun.* **1977**, *23*, 421.
(19) (a) Fan, F.-R. F.; Bard, A. J. *J. Am. Chem. Soc.* **1980**, *102*, 3677. (b) Tanaka, S.; Bruce, J. A.; Wrighton, M. S. *J. Phys. Chem.* **1981**, *85*, 3778.
(20) (a) Ellis, A. B.; Kaiser, S. W.; Bolts, J. M.; Wrighton, M. S. *J. Am. Chem. Soc.* **1977**, *99*, 2839. (b) Minoura, H.; Watanabe, T.; Oki, T.; Tsuiki, M. *Jpn. J. Appl. Phys.* **1977**, *16*, 865. (c) Minoura, H.; Tsuiki, M.; Oki, T. *Ber. Bunsenges. Phys. Chem.*, **1977**, *81*, 588. (d) Ginley, D. S.; Butler, M. A. *J. Electrochem. Soc.* **1978**, *125*, 1968. (e) Gobrecht, J.; Tributsch, H.; Gerischer, H. *Ibid.* **1978**, *125*, 2085. (f) Calabrese, G. S.; Wrighton, M. S. *J. Am. Chem. Soc.* **1981**, *103*, 6273.
(21) (a) Chambers, J. A. In "The Chemistry of the Quininoid Compounds"; Patai, S., Ed.; Wiley: New York, 1974; pp 756–759. (b) Decker, F.; Parkinson, B. A. *J. Electrochem. Soc.* **1980**, *127*, 2370.
(22) Pankove, J. I.; Pollack, F. H.; Schnabolk, C. *J. Non-Cryst. Solids* **1980**, *35*, 459.

A photoacoustic spectrum of a mixture of powdered MgO and a-Si:H, scraped from the stainless steel, is also shown in Figure 3. The onset is not well defined, but significant absorption does not occur until about 800 nm, from which point it shows a steady increase, in resonable agreement with published absorption spectra of a-Si:H samples prepared by decomposition of SiH_4 in a DC glow discharge.[3a]

Clearly, the Φ_e vs. wavelength curve contrasts with the photoacoustic spectrum. The cause of the short wavelength defect found with these photoelectrodes is not certain; however, it is likely to be related to the low penetration depth (200–300 Å) of blue light which results from the high absorptivity of $\sim 10^6$ cm^{-1} of a-Si:H for high-energy visible light.[3a] Defects in short-wavelength response have been noted previously for photoelectrodes which have suffered surface damage, introducing traps and recombination centers at and near the surface.[23] The photoaction spectrum of the 8000-Å thick intrinsic a-Si:H layer is similar to the spectral response reported by others[8b,24] for solid-state p–i–n photovoltaic cells with an intrinsic a-Si:H layer thickness of about 5000 Å; both show a peak near 600 nm and a decline in response at higher energy. This suggests the problem is intrinsic to a-Si:H and not the result of surface treatment or unique interactions introduced at the a-Si:H/electrolyte interface.

The spectral response for a-Si:H photocathodes shown in Figure 3 indicates that the quantum yields determined at 633 and 514 nm in steady-state measurements (vide infra) are near optimum, but do not represent the maximum values obtainable. Nonetheless, it is clear that the device does respond over a large fraction of the solar spectrum.

Steady-State Characteristics. a-Si:H photocathode-based cells can be used to convert optical energy to electricity with modest efficiencies in both aqueous and nonaqueous media, as indicated in Table II. In such cases the uphill reduction effected at the photocathode is reversed at the counterelectrode resulting in no net chemical change in the device. The steady-state, open-circuit photovoltages are consistent with the results obtained by cyclic voltammetry in CH_3CN. The largest photovoltages are obtained in CH_3CN/0.1 M $[n\text{-}Bu_4N]BF_4$/10 mM $Ru(bpy)_3^{2+/+}$ solutions poised to −1.4 V vs. SCE (~700 mV) while $BAQ^{0/-}$, which gives anomalous results by cyclic voltammetry, yields a lower E_V(oc) (~400 mV) than would be expected based on the E_V's from redox couples having the same $E_{1/2}$. The consistency of these findings supports the validity of mapping out the interface energetics of these thin film, intrinsic materials using cyclic voltammetry.

Decamethylferricenium/decamethylferrocene is the most positive couple employed in steady-state experiments and was examined in absolute C_2H_5OH as this solvent has been found to enhance the stability of a-Si:H[4] and single-crystal n-Si photoanodes.[25] In a ~10 mM decamethylferricinium solution poised to −0.32 V, the a-Si:H photocathodes are quite durable when illuminated with white light at ~80 mW/cm², giving a constant current output (~1 mA/cm²) for ~50 h when potentiostatted at −0.1 vs. SCE. After this period the current–voltage characteristics were unchanged. Unfortunately, the conversion efficiencies are fairly low, apparently as a result of the low Φ_e, in part due to absorption of the light by the redox couple.

In aqueous solution the PVS couple can be used in a-Si:H photocathode-based cells giving efficiencies comparable to single-crystal p-Si in CH_3CN/H_2O mixtures in the presence of methyl viologen.[13,26] Current–time curves indicate that the a-Si:H photocathodes are durable for 5–10 h in 0.5 M PVS, 0.5 M KCl solutions at a photocurrent density of ~2.2 mA/cm². A decline in photocurrent generally occurs after this period. The decay is a result of separation of the a-Si:H thin film from the stainless steel substrate, a process which can also occur when electrodes

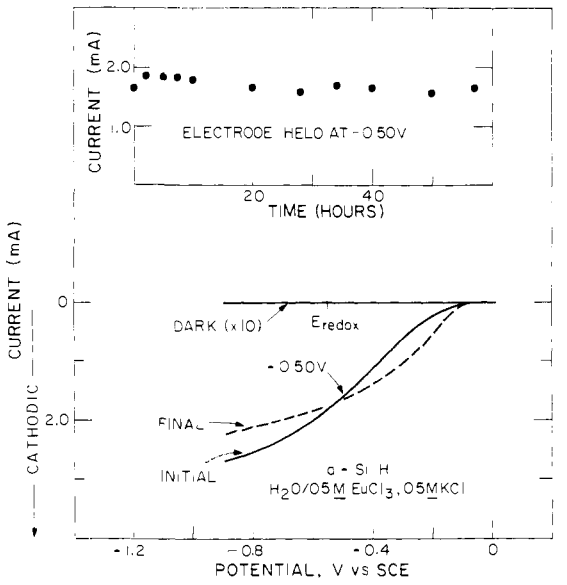

Figure 4. Steady-state photocurrent–voltage curves for an a-Si:H photocathode in aqueous solution, pH 6, before (—) and after (---) potentiostatting the illuminated electrode at −0.50 V (inset). White light illumination is at ~80 mW/cm².

are stored in distilled water in the dark for several days. Both low pH and Cl^- ion appear to accelerate this phenomenon, but it does not occur at the same rate with all electrodes. We believe that this problem results from high stresses at the p^+-a-Si:H/stainless steel interface. Acceleration of the decomposition by aqueous solutions may be a result of attack on the substrate through pinholes that could be present in such thin layers. We note that on a partially separated electrode, regions which are still in contact with the substrate show no decline in output characteristics, and that the thicker (~4 μm) a-Si:H photoanodes previously examined[4] do not exhibit this behavior.

The $Eu^{3+/2+}$ couple has proven useful at p-GaP electrodes[27] and is appealing, since it is an optically transparent redox couple. For a-Si:H photocathodes the efficiencies (~2 to 3%) are comparable to the other redox couples examined. A small pH dependence is found, consistent with slightly more positive band-edge positions at lower pH. At pH 6 the electrode proved quite durable in the $Eu^{3+/2+}$/electrolyte solution, as shown by data in Figure 4. Operation for about 50 h at ~3.2 mA/cm² caused a small decline in the maximum Φ_e, but the fill factor shows some improvement. After this period the electrode was examined in CH_3CN/0.1 M $[n\text{-}Bu_4N]BF_4$/1 mM MV^{2+} by cyclic voltammetry and showed an E_V of 650 mV for the $MV^{2+/+}$ wave. Subsequent etching for 5 s in 5% HF improved this to its initial value of ~700 mV. The results indicate that the a-Si:H photocathodes can be durable if problems related to adhesion to the substrate can be solved.

Most of the redox systems examined show resonable efficiencies (2 to 4%) and respectable values of Φ_e at low light intensities. The values of Φ_e are not corrected for solution absorption or surface reflectivity. These losses amount to ~30% under the conditions employed. Unfortunately, there is a serious decline in efficiency as solar light intensities are approached. As light intensity is increased there is a decrease in Φ_e and fill factor which suggests that recombination centers and/or resistivity of the interface or bulk material are limiting the device properties (Table II). The fairly thin intrinsic layer employed would seem to rule out bulk resistivity problems, thus focusing attention on difficulties at the interface. A similar decline in output characteristics as light intensity is increased is found with single-crystal Si photoelectrochemical cells.[9,13,26]

Surface Modification and H_2 Evolution. The evolution of H_2 from photocathodes for use as a storable fuel is a desirable ob-

(23) Heller, A.; Chang, K.-C.; Miller, B. *J. Electrochem. Soc.* **1977**, *124*, 697; *J. Am. Chem. Soc.* **1978**, *100*, 684.
(24) Cretella, M. C.; Gregory, J. A. *J. Electrochem. Soc.* **1982**, *129*, 2850.
(25) Legg, K. D.; Ellis, A. B.; Bolts, J. M.; Wrighton, M. S. *Proc. Natl. Acad. Sci. U.S.A.* **1977**, *74*, 4116.
(26) Bookbinder, D. C.; Lewis, N. S.; Bradley, M. G.; Bocarsly, A. B.; Wrighton, M. S. *J. Am. Chem. Soc.* **1979**, *101*, 7721.
(27) Memming, R. *J. Electrochem. Soc.* **1978**, *125*, 117.

Table II. Output Parameters for a-Si:H Photoelectrochemical Cells

electrolyte system (light source)[a]	input power, mW (power density, mW/cm²)	Φ_e[b] at E_{redox} (mA/cm² at E_{redox})	E_V(oc),[c] mV (E_V at η_{max}, mV)	η_{max},[d] %	fill factor[e]
CH_3CN/0.1 M [n-Bu_4N]ClO_4/10 mM $Ru(bpy)_3^{2+/+}$	1.0 (6)	0.28	700 (300)	3.2	0.32
E_{redox} = −1.4 V vs. SCE	2.0 (12)	0.24	700 (300)	2.7	0.32
(632.8 nm)	3.4 (21)	0.23	740 (300)	2.5	0.29
CH_3CN/0.1 M [n-Bu_4N]ClO_4/0.1 M BAQ	0.20 (1.0)	0.26	410 (200)	2.0	0.38
E_{redox} = −0.87 V vs. SCE	0.50 (2.5)	0.25	430 (200)	1.8	0.33
(632.8 nm)		0.23	430 (200)	1.6	0.31
CH_3CN/0.1 M [n-Bu_4N]ClO_4/10 mM [decamethylferrocene]$^{+/0}$	1.0 (6)	0.15	320 (200)	0.7	0.32
E_{redox} = 0.06 V vs. SCE	2.0 (12)	0.16	360 (200)	0.7	0.28
(514 nm)	4.0 (24)	0.16	380 (200)	0.7	0.26
H_2O/0.1 M KCl/0.1 M PVS	0.28 (4)	0.30	360 (200)	2.8	0.29
E_{redox} = −0.38 V vs. SCE	0.85 (12)	0.25	400 (200)	2.5	0.28
(632.8 nm)	1.73 (25)	0.21	420 (200)	2.3	0.25
H_2O/0.5 M KCl/0.5 M $EuCl_3$ pH 6	0.098 (1.0)	0.39	450 (230)	3.2	0.36
E_{redox} = −0.62 V vs. SCE	0.80 (8.4)	0.39	530 (230)	3.3	0.31
(632.8 nm)	2.91 (30.3)	0.32	580 (210)	1.8	0.20
H_2O/0.5 M KCl/0.5 M $EuCl_3$ pH 1	0.80 (8.3)	0.42	620 (290)	4.2	0.31
E_{redox} = −0.62 V vs. SCE	2.85 (29.6)	0.32	670 (240)	2.4	0.21
(632.8 nm)					
H_2O/0.5 M KCl/0.5 M $EuCl_3$ pH 6	(16)	(1.87)	540 (220)	1.6	0.25
E_{redox} = −0.62 V vs. SCE	(28)	(3.26)	560 (220)	1.5	0.23
white light	(95)	(7.20)	660 (200)	0.8	0.16
H_2O/0.5 M KCl/0.5 M $EuCl_3$ pH 1	(16)	(2.10)	660 (300)	2.6	0.30
E_{redox} = −0.62 V vs. SCE	(28)	(3.46)	670 (300)	2.3	0.27
white light	(95)	(9.57)	690 (240)	1.2	0.18

[a] Lasers were used for a monochromatic source, as described in the Experimental Section. [b] Quantum yield for electron flow at E_{redox}. Data are uncorrected for reflection or solution absorption. Current density at E_{redox} given for a white-light source. [c] Photovoltages; E_V(oc) is the difference in onset of photocurrent and E_{redox}. E_V at η_{max} is the difference between the potential at the maximum power point and E_{redox}. [d] η_{max} is defined as $\eta_{max} = [(E_V \times i)_{max}/\text{optical power in}] \times 100\%$. [e] Fill factor is defined as $(E_V \times i)_{max}/E_V(oc) \times i_{sc}$ is current at short circuit.

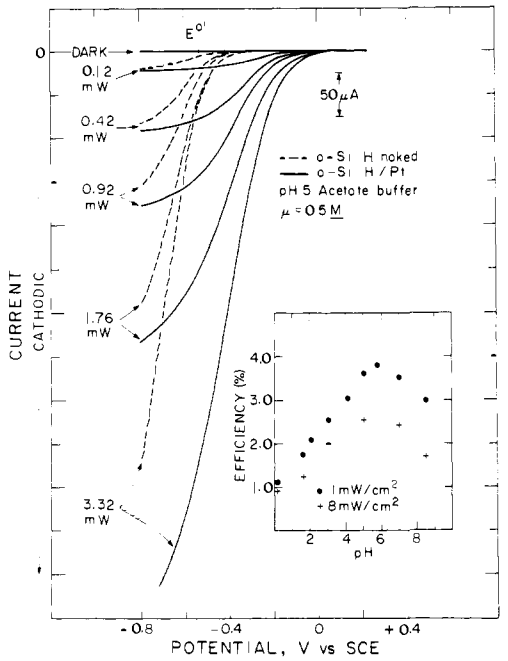

Figure 5. Steady-state photocurrent–voltage curves for a naked (---) and platinized (—) a-Si:H photocathode (1×10^{-8} mol/cm² Pt) at pH 5. Data from these curves are given for electrode 2 in Table III. Inset shows efficiency as a function of pH for electrode 1 at 2.5×10^{-8} mol/cm² Pt coverage.

jective. Unfortunately, as has been found with most photoelectrodes, the a-Si:H surface is a poor H_2 cathode. In Figure 5 it can be seen that a small photovoltage is obtained for H_2 production, but an overvoltage is required to drive the reaction at a light intensity limited rate. It is noteworthy that this response is better than that obtained at naked crystalline p-Si,[9,13,26] for which little or no photovoltage is observed.

Table III. Output Parameters for H_2 Evolution at a-Si:H Photocathodes[a]

electrode/ catalyst	input power[b] (power density, mW/cm²)	Φ_e at E_{redox}	E_V(oc), mV (E_V at η_{max}, mV)	η_{max}, %	fill factor
1	0.123 (1.0)	0.35	535 (335)	3.7	0.38
Pt, 2.5×10^{-8} mol/cm²	1.00 (7.9)	0.26	625 (235)	1.7	0.20
pH 5	3.64 (29.0)	0.15	665 (215)	0.8	0.16
2	0.115 (0.9)	0.34	535 (195)	2.2	0.24
Pt, 1×10^{-8} mol/cm²	0.92 (7.3)	0.31	560 (165)	1.5	0.17
pH 5	3.32 (26.4)	0.28	620 (175)	1.2	0.14
2	0.115 (0.9)	0.26	555 (275)	2.2	0.30
Pt, 6×10^{-8} mol/cm²	0.92 (7.3)	0.24	580 (220)	1.7	0.24
pH 5	3.32 (26.4)	0.23	615 (215)	1.4	0.20
3	1.0 (4)	0.31	600 (280)	2.8	0.29
$[(PQ^{2+})_n/Pt]_{surf.}$	2.0 (8)	0.29	600 (280)	2.5	0.28
pH 4.0	4.3 (17)	0.30	600 (280)	2.3	0.25
4	1.0 (5)	0.29	600 (280)	2.8	0.31
$[(PQ^{2+})_n/Pd]_{surf.}$	2.0 (10)	0.29	600 (280)	2.8	0.31
pH 4.0	5.0 (25)	0.29	600 (280)	2.6	0.27

[a] Parameters are as defined in Table II. [b] Input power at 632.8 nm.

Previously we[9,12,28,29] and and others[14,30] have employed several schemes for the improvement of multielectron inner-sphere electrode reactions at semiconductor surfaces. Deposition of Pt

(28) Simon, R. A.; Ricco, A. J.; Harrison, D. J.; Wrighton, M. S. *J. Phys. Chem.*, in press.
(29) Calabrese, G. S.; Buchanan, R. M.; Wrighton, M. S. *J. Am. Chem. Soc.* **1982**, *104*, 5786.
(30) (a) Abrūna, H. D.; Bard, A. J. *J. Am. Chem. Soc.* **1981**, *103*, 6898. (b) Thompson, L.; DuBow, J.; Rajeshwar, K. *J. Electrochem. Soc.* **1982**, *129*, 1934. (c) Fan, F.-R. F.; Hope, G. A.; Bard, A. J. *Ibid.* **1982**, *129*, 1647. (d) Fan, F.-R. F.; Keil, G.; Bard, A. J.; submitted for publication.

onto the photocathode surface is one workable approach.[9,14] The improvement in H_2 evolution efficiency which results from direct platinization is indicated in Figure 5, and data are summarized in Table III. The optimum coverage of Pt lies in the 1 to 5 × 10^{-8} mol/cm^2 range, varying slightly from electrode to electrode. These surfaces show a dependence of efficiency on pH (inset of Figure 5), indicating that the interface energetics remain controlled by the solution potential. The pH profile shows an optimum at a pH of 5 to 6 which probably arises from the shift of $E^{\circ\prime}(H_2O/H_2)$ to more negative potentials, resulting in improved $E_V(oc)$ and better charge separation due to increased band bending. A large work function metal such as Pt might be expected to contact the valence band of a-Si:H,[18] resulting in an ohmic contact to the photocathodes used here. However, as found with single-crystal p-Si[9a] the electrodeposition of Pt results in substantial photovoltages, indicating the contact is not ohmic. In order to form good ohmic contacts on p-Si, though, high temperatures ($T > 200$ °C) are required in order to obtain platinum silicide formation.[31] Good barriers for platinized p-type semiconductors in contact with aqueous H_2/H_2O have recently been attributed to hydriding of the Pt to lower its work function.[14e] Electron microscopy and XRF analysis shows that Pt is deposited in an island formation and that most of the a-Si:H surface remains exposed to solution. The Pt deposits behave phenomenologically as catalyst sites for H_2O reduction. Platinized a-Si:H photocathodes give about the same fill factor as do naked electrodes, showing that the Pt does not diminish problems associated with near-surface recombination.

The derivatization of electrodes with reagent I and subsequent metallization is a second modification procedure leading to improved H_2 evolution output parameters.[9] In this case the a-Si:H/polymer interface, not the a-Si:H/M interface, defines the energetics. Surface attachment of a polymer from I, $[(PQ^{2+})_n]_{surf.}$, at coverages in the range 1 to 5 × 10^{-8} mol/cm^2 is effected by potentiostatting the electrode in aqueous solutions of I at potentials where the monomer is reduced to the radical cation. The cyclic voltammetry for a derivatized a-Si:H photocathode is shown in Figure 6a and compared with the response at a derivatized, reversible W electrode. The cyclic voltammetry waves are associated with the $[(PQ^{2+})_n]_{surf.} \rightleftarrows [(PQ^{+})_n]_{surf.}$ interconversion. For scan rates up to ~50 mV/s and coverages of 1 to 5 × 10^{-8} mol/cm^2, the peak current for reduction varies linearly with scan rate at the photoelectrode as expected for a surface-confined species.[32] The extent to which $[(PQ^{2+})_n]_{surf.}$ can be reduced in an uphill sense on the a-Si:H is ~700 mV, the difference in cathodic current peak on W and illuminated a-Si:H, and accords well with the data in Figure 2. The potential $E^{\circ\prime}$ of the $[(PQ^{2+/+})_n]_{surf.}$ is −0.55 ± 0.05 V vs. SCE[9] and the photovoltage is as would be found for a solution couple with this $E^{\circ\prime}$.

The surface-confined $(PQ^{2+})_n$ polymer provides a convenient method to explore the effect of light intensity and pH on the steady-state E_V obtainable. Slow potential scanning (1 to 5 mV/s) produces nearly zero peak-to-peak separation for the oxidation and reduction corresponding to $[(PQ^{2+})_n]_{surf.} \rightleftarrows [(PQ^{+})_n]_{surf.}$. We then take the peak position relative to the position on derivatized W as a measure of the steady-state, open-circuit photovoltage. In aqueous 0.1 M KCl solution $E_V(oc)$ shows an increase of about 90 mV as the light intensity of the 514-nm Ar ion laser line is increased from ~3 to ~1500 mW/cm^2. A plot of E_V vs. log of the light intensity is nearly flat (above 100 mW/cm^2 of 514.5-nm light) and indicates that the photovoltage saturates at fairly low light intensities. The pH dependence of E_V was examined in a similar fashion, as done previously for single-crystal p-Si derivatized with I. We find a small increase in E_V of ~15 mV per pH unit as the pH is lowered from 9 to 3 for the derivatized surface, consistent with the solution results for PVS (vide supra). This may be attributed to protonation reactions of a thin native

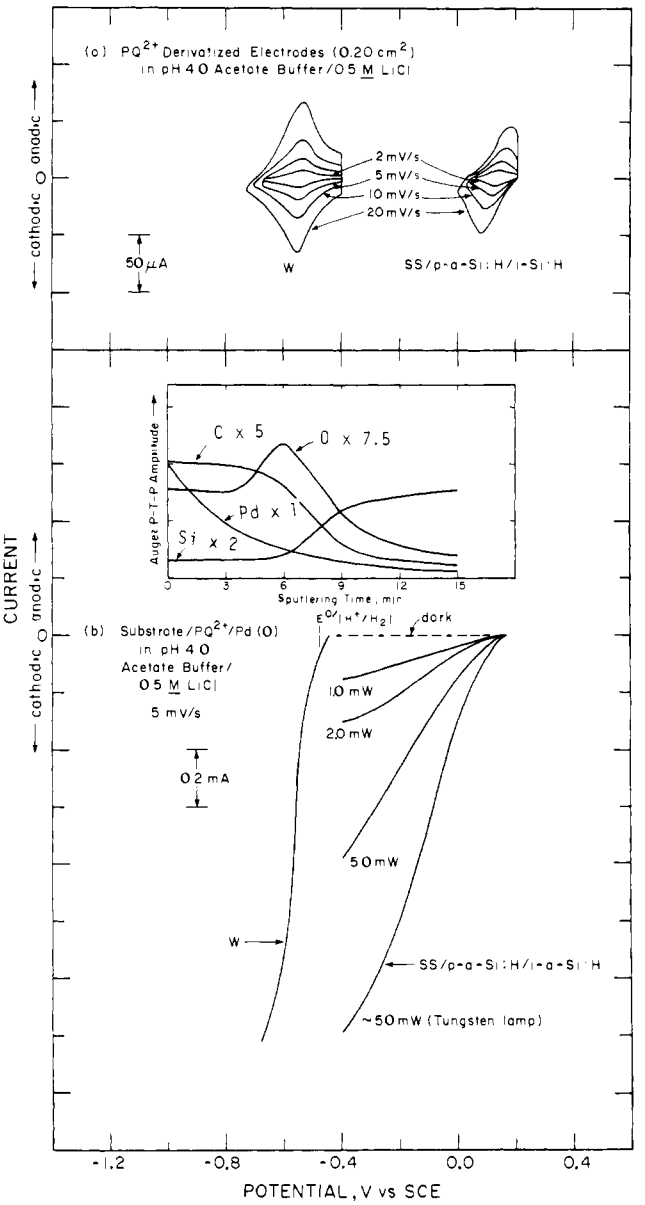

Figure 6. (a) Cyclic voltammetry of surface confined $[(PQ^{2+})_n]_{surf.}$ as a function of scan rate on W and an illuminated (633 nm) a-Si:H photocathode in aqueous solution. (b) Steady-state current–voltage curves for substrate/$[(PQ^{2+})_n$/Pd$]_{surf.}$ electrodes at pH 4, comparing response at surface modified W and a-Si:H of equal area. Illumination is at 633 nm at lower intensities, white light source at ~50 mW input. Inset shows the Auger depth profile for the same a-Si:H/$[(PQ^{2+})_n$/Pd$]_{surf.}$ electrode after H_2 evolution. O signal is enhanced for clarity.

oxide on a-Si:H,[18b,33] as has been shown to be the case for the small shift in flat-band potential with pH found for single-crystal Si.[9b] The $E^{\circ\prime}[(PQ^{2+/+})_n]_{surf.}$ is independent of pH.

Unlike the W or W/$[(PQ^{2+})_n]_{surf.}$ interfaces which have a significant overpotential for H_2 evolution, the electrodeposition of Pt or Pd (~10^{-8}–10^{-7} mol/cm^2) onto the $[(PQ^{2+})_n]_{surf.}$ results in a W/$[(PQ^{2+})_n$/M$]_{surf.}$ electrode/catalyst system capable of evolving H_2 at pH values where the $[(PQ^{2+/+})_n]_{surf.}$ system is thermodynamically able to reduce water. The pH response of such interfaces and their structure have been reported previously.[9] The $[(PQ^{2+})_n$/Pt$]_{surf.}$ system has been shown to operate at peak efficiencies at a pH of about 4 on single-crystal p-Si. This pH, where $E^{\circ\prime}(H_2O/H_2) = -0.48$ V vs. SCE, allows ~70 mV of driving force for the noble metal mediated reduction of H_2O by the $[(PQ^{2+/+})_n]_{surf.}$, since $E^{\circ\prime}[(PQ^{2+/+})_n]_{surf.}$ is somewhat more negative

(31) Milnes, A. G.; Feucht, D. L. "Heterojunctions and Metal-Semiconductor Junctions"; Academic Press: New York, 1972; p 185.
(32) Smith, D. F.; William, K.; Kuo, K.; Murray, R. W. *J. Electroanal. Chem.* **1979**, *95*, 217.
(33) Richter, H.; Schroder, B.; Geiger, J. *J. Non-Cryst. Solids* **1981**, *43*, 153.

than $E^{\circ\prime}(H_2O/H_2)$ at pH 4. The electrodeposition of Pt or Pd onto the a-Si:H/$[(PQ^{2+})_n]_{surf.}$/solution interface results in an electrode capable of producing H_2 with reasonable efficiencies (Table III and Figure 6). The Auger/depth profile analysis (Figure 6b) locates most of the Pd at the polymer/solution interface and is in reasonable agreement with data previously published on such structured interfaces.[9b] Note that the presence of an oxide layer at the a-Si:H surface is indicated by the Auger analysis. At low intensities the efficiencies obtained with modified a-Si:H electrodes are about 3%, slightly lower than the ~5% found for similarly modified p-Si single crystals, but efficiency declines more rapidly than for single crystals as the light intensities are increased. The photoelectrode is capable of operating at current densities similar to the W/$[(PQ^{2+})_n$/Pd$]_{surf.}$ electrodes at high light intensities (~200 mW/cm^2) (Figure 6b). The result shows that the catalyst system eventually becomes the current-limiting factor.

We find that the durability of H_2-evolving electrochemical cells based on the a-Si:H/$[(PQ^{2+})_n$/M$]_{surf.}$ photoelectrodes is comparable to that obtained previously with this surface-confined catalyst. One mode for catalyst deactivation over time has been identified as heavy-metal poisoning, such as Pb or Hg, of the noble metal.[9b] Although current–time runs were done in carefully prepared, preelectrolyzed solutions of 1 mM H_2SO_4, as described in the Experimental Section, the current output of a surface-modified photoelectrode potentiostatted at +0.4 V vs. a Pt/H_2 reference declined steadily over a 24-h period to ~$^1/_8$ its initial value. This decline was also observed with a W/$[PQ^{2+})_n$/Pt$]_{surf.}$ electrode held at −0.06 V vs. Pt/H_2 for 24 h. Usually the currents of deactivated electrodes are regenerated to original values by the electrodeposition of more Pt or Pd. Thus, we conclude that the photoelectrode is not the major source of instability over this time scale in these cells; rather the problem lies with catalyst deactivation.

Summary

The large photovoltages reported here demonstrate that good Schottky barriers may be obtained at the a-Si:H/electrolyte interface when the back contact to the intrinsic material is made via the valence band with a heavily doped p^+ layer. We find that the a-Si:H photocathodes are more rugged at positive potentials than single-crystal p-Si electrodes, and long-term durability (~50 h) has been demonstrated in aqueous and nonaqueous electrolyte solutions. At the a-Si:H surface H_2 evolution can be catalyzed using techniques previously applied to single-crystal materials demonstrating that a relatively inexpensive, thin-film (<20 000 Å) device made from abundant elements can be utilized for the generation of H_2 at efficiencies only somewhat lower than found for more expensive single-crystal p-Si-based devices.

When corrected for reflection and solution absorption, the maximum quantum yield for electron flow can be relatively high (~0.65 at λ_{max} = 580 nm) indicating that charge separation is readily effected upon photoexcitation of electrons in the a-Si:H when there is a field across the material. The decline in Φ_e observed at short wavelengths suggests that there are difficulties in charge separation and transport in the near surface region of a-Si:H. The fill factors from a-Si:H photocathodes are lower than from single-crystal p-Si photocathodes, offsetting the advantage associated with the large photovoltage from a-Si:H. It is possible that the low fill factors found for a-Si:H are due to the much thicker space charge region which develops in the intrinsic layer, resulting in lower electric field strength than is usually observed at doped semiconductor/electrolyte junctions. While the intrinsic material has the advantage of a thick field region from the standpoint that carriers are generated in a field region throughout the absorbing layer, light doping of the a-Si:H to obtain a thinner space charge layer, and hence higher electric field strength, might improve the device characteristics of photoelectrochemical cells.

Acknowledgment. Work at M.I.T. was supported by the U.S. Department of Energy, Office of Basic Energy Sciences, Division of Chemical Sciences. D.J.H. acknowledges support as a NSERC of Canada Fellow and A.J.R. acknowledges support as an M.I.T. NPW Fellow, 1982–1983. Use of the Central Facilities of the M.I.T. Center for Materials Science and Engineering is gratefully acknowledged.

Registry No. I, 74173-49-2; H_2, 1333-74-0; PVS, 77951-49-6; H_2O, 7732-18-5; Pd, 7440-05-3; Pt, 7440-06-4; Si, 7440-21-3; $EuCl_3$, 10025-76-0; Ru(2,2′-bipyridine)$_3$, 74391-32-5; [Ru(2,2′-bipyridine)$_3$]$^-$, 56977-23-2; [BAQ]$^-$, 77898-33-0; [BAQ]$^{2-}$, 85719-02-4; [Ru(2,2′-bipyridine)$_3$]$^+$, 56977-24-3; [Ru(2,2′-bipyridine)$_3$]$^{2+}$, 15158-62-0; [*N*,*N*′-bis(3-propylsulfonate)-4,4′-bipyridinium]$^-$, 79008-86-9; [*N*,*N*′-bis(3-propylsulfonate)-4,4′-bipyridinium]$^{2-}$, 85719-03-5; [BAQ]$^+$, 85719-04-6; [MV]$^+$, 25239-55-8; MV, 25128-26-1; [Ru(acac)$_3$]$^-$, 66560-52-9; [Ru(acac)$_3$]$^{2-}$, 85701-89-9; [MV]$^{2+}$, 4685-14-7; [TCNQ]$^-$, 34507-61-4; [TCNQ]$^{2-}$, 66701-41-5; [decamethylferrocene]$^+$, 54182-41-1; decamethylferrocene, 12126-50-0; [pentamethylferrocene]$^+$, 81064-27-9; pentamethylferrocene, 63074-30-6; TCNQ, 1518-16-7; [ferrocene]$^+$, 12125-80-3; ferrocene, 102-54-5; [acetylferrocene]$^+$, 32662-25-2; acetylferrocene, 1271-55-2; CH_3CN, 75-05-8; [*n*-Bu_4N]BF_4, 429-42-5; 4,4′-bipyridine, 553-26-4; 1,3-propanesulfone, 1120-71-4; KCl, 7447-40-7; BAQ, 84-47-9.